Information Fusion 64 (2020) 194–204

Contents lists available at ScienceDirect

Information Fusion

journal homepage: www.elsevier.com/locate/inffus

Unscented kalman filter with process noise covariance estimation for vehicular ins/gps integration system

Gaoge Hu [a,*], Bingbing Gao [a], Yongmin Zhong [b], Chengfan Gu [b]

[a] School of Automation, Northwestern Polytechnical University, Xi'an, China
[b] School of Engineering, RMIT University, Bundoora, VIC 3083, Australia

ARTICLE INFO

Keywords:
Vehicular navigation
Ins/gps integration
Unscented kalman filter
Process noise covariance
And maximum likelihood estimation

ABSTRACT

The unscented Kalman filter (UKF) has proved to be a promising methodology to integrate INS and GPS for vehicular navigation. Nevertheless, the disturbance suppression of system noise uncertainty on the UKF performance is still an open issue. In this paper, based on the maximum likelihood (ML) principle, a new adaptive UKF with process noise covariance estimation is proposed to enhance the UKF robustness against process noise uncertainty for vehicular INS/GPS integration. The proposed method extends the concept of ML estimation from the linear Kalman filter to the nonlinear UKF to estimate the process noise covariance. Meanwhile, an estimation window for fixed-length memory is introduced to emphasize the use of the new observations and gradually discard the old ones. Since it has the capability to estimate and update the process noise covariance online, the proposed method improves the standard UKF by restraining the disturbance of process noise uncertainty on the filtering solution. The effectiveness and superiority of the proposed method have been verified through Monte Carlo simulations and practical experiment in vehicular INS/GPS integration system.

1. Introduction

The inertial navigation system (INS) is a completely autonomous unit which calculates the attitude, velocity and position of a vehicle with the output of inertial sensors. However, due to the drift of inertial sensors, its navigation error grows unboundedly with time [1]. On the contrary, the global position system (GPS) is able to provide accurate velocity and position for a long-term period. However, GPS has a low data update rate and its performance depends on external environment and satellite accessibility, leading to the difficulty in achieving continuous navigation information [2]. Given the complementary characteristics, the integration of INS and GPS enables to sufficiently exploit the individual advantages of both standalone systems and obtains an optimistic solution to enhance the navigation accuracy [2-5].

INS/GPS integration is a nonlinear system in essence [6]. In some cases requiring a particular focus on real-time performance, the nonlinear system can be linearized by assuming the initial state estimate involves small error in order to reduce the computational cost. Nevertheless, in most practical applications, it is difficult to satisfy this assumption, especially for vehicular navigation in which low-performance inertial sensors are commonly used [7]. Therefore, INS/GPS integration has to employ a nonlinear model to describe the complete propagation process of system error and reflect real system characteristics. As a result, a nonlinear filter is required for navigation sensor fusion [6-8].

The extended Kalman filter (EKF) is a widely used method for INS/GPS integration. It extends the linear Kalman filter [9] to a nonlinear system by linearization of the nonlinear system model via the first-order Taylor expansion [10]. However, the first-order linearization of system model may cause a biased or even divergent filtering solution. Moreover, EKF also requires the calculation of the Jacobian matrix, which is a cumbersome process [11]. Even though the sequential Monte Carlo based method, where the particle filter is a typical example, is also useful to state estimation in nonlinear systems, it is expensive in computation, especially for high-dimensional systems [12]. The unscented Kalman filter (UKF), which has received attention in many areas such as aerospace navigation [2], target tracking [13] and system identification [14,15], is proposed to overcome the weaknesses of EKF. It is a derivative-free method which uses a finite number of sigma points to capture higher-order statistics of the system, leading to a better performance than EKF in terms of both estimation accuracy and convergence [7,11]. However, similar to EKF, a major difficulty in designing

* Corresponding author.
E-mail address: hugaoge1111@126.com (G. Hu).

https://doi.org/10.1016/j.inffus.2020.08.005
Received 4 January 2019; Accepted 3 August 2020
Available online 6 August 2020

UKF for INS/GPS integration is its high dependence on the prior statistical information of the process and measurement noises. If inaccurate noise statistics are used, the UKF performance will be degraded [16,17].

Note that the statistical characteristics of system noise actually describe the uncertainty associated with system dynamics. Compared with the measurement model, whose accuracy can be guaranteed using high-precision measurement equipment together with plenty of available measurement data [18], the process model is just a theoretical approximation to the real-world system [19-21]. The intrinsic coupling of process noise and system dynamics makes it more difficult to determine the process noise covariance than that of the measurement noise covariance, and the achieved result is inevitably involves errors [22]. For the vehicular INS/GPS integration, it has also been proved by field tests and analysis that the navigation performance is mainly subject to the inherent process noise uncertainty as GPS works normally [23]. Therefore, it is required the UKF have the capability to restrain uncertainty involved in process noise covariance when it is applied to the vehicular INS/GPS integration.

Although the adaptive Kalman filters based on linear system is able to provide robustness filtering solutions against process model uncertainty [24,25], they cannot be applied to nonlinear INS/GPS integration systems due to the theoretical limitations. Recently, various methods were reported to handle the influence of inaccurate system noise covariance on the UKF estimation. Cho and Choi reported a method by using receding horizon to adaptively restrain model uncertainty, leading to the improved UKF robustness [26]. However, this method suffers from a poor convergence, due to the use of a finite impulse response structure. Song and Han presented an adaptive UKF to update the covariance of process noise by minimizing the difference between the computed and actual innovation covariances [27]. However, this method requires the calculation of partial derivatives, causing a relatively large computational burden. Soken and Hajiyev studied an adaptive fading UKF to weaken the influence of process noise uncertainty by introducing a scale factor to adjust the Kalman gain matrix [20]. However, since the scale factor is determined empirically, it may lead to a suboptimal or biased filtering solution. Based on the covariance matching technique, Meng et al. reported an adaptive UKF to online estimate and adjust the noise covariance using the innovation and residual sequences [28]. However, the use of the covariance matching technique yields a steady-state estimation error, leading to a limited improvement in the filtering accuracy. Based on the adaptive robust Kalman filter [29], an adaptive robust UKF (ARUKF) was developed by incorporating an adaptive factor in the robust UKF to restrain the disturbance of system noise uncertainty on the UKF solution [30]. However, the empirical determination of the equivalent weight factor and adaptive factor also limits its usage on some special cases.

Maximum likelihood (ML) estimation, as the name might imply, is a method to estimate the unknown parameters of a statistical model by maximizing the likelihood function of unknown parameters and a given set of measurements [31,32]. The ML solution is unique and converged in the probabilistic sense [31]. It is also unbiased in terms of minimum covariance under independent and identically distributed measurements. Because of these advantages, the concept of ML has been used for adaptive filtering [31-34]. However, all the existing ML based filtering methods are derived in the framework of linear system, unsuitable for nonlinear state estimation. Due to the difficulty in theoretical derivation, there has been very limited research on using the ML estimation to improve the UKF performance in the presence of inaccurate noise covariance for nonlinear state estimation.

This paper presents a new maximum likelihood based adaptive UKF (MLAUKF) to handle the uncertainty involved in process noise covariance for vehicular INS/GPS integration. MLAUKF constructs the conditional probability density of measurement using the statistical information of innovation vector. Afterwards, it estimates the covariance matrix of the process noise based on the ML principle and subsequently feeds the obtained estimations back to UKF to adjust the Kalman gain. MLAUKF innovatively extends the concept of ML estimation from the linear Kalman filter to the nonlinear UKF to adapt the process noise covariance. And different with the existing studies [32,33], it also introduces an estimation window for fixed-length memory to fully use the new observations and gradually discard the old ones. By estimating and updating process noise covariance online, MLAUKF improves the UKF robustness against process noise uncertainty. Monte Carlo simulations, experiments and comparison analysis have been conducted to comprehensively evaluate the performance of the proposed method for vehicular navigation.

2. Mathematical models for ins/gps integration

In this section, the mathematical models for INS/GPS integration are established. Specifically, the process model is established by combining the INS error equation with the inertial sensors' error equation, and the measurement model is constructed by using the difference between INS and GPS in terms of velocity and position.

2.1. Process model

The navigation frame (n-frame) is selected as the E-N-U (East-North-Up) geography frame. Denote the inertial frame by *i*, the earth frame *e*, the body frame *b* and the INS simulated actual platform frame n'. The nonlinear attitude and velocity error equations with large initial estimation error can be formulated as [8]

$$\begin{cases} \dot{\boldsymbol{\phi}} = \boldsymbol{C}_{\omega}^{-1}\left[\left(\boldsymbol{I}-\boldsymbol{C}_{n}^{n'}\right)\hat{\boldsymbol{\omega}}_{in}^{n}+\boldsymbol{C}_{n}^{n'}\delta\boldsymbol{\omega}_{in}^{n}-\boldsymbol{C}_{b}^{n'}\delta\boldsymbol{\omega}_{ib}^{b}\right] \\ \delta\dot{\boldsymbol{v}}^{n} = \left[\boldsymbol{I}-\left(\boldsymbol{C}_{n}^{n'}\right)^{T}\right]\boldsymbol{C}_{b}^{n'}\hat{\boldsymbol{f}}^{b}+\boldsymbol{C}_{b}^{n}\delta\boldsymbol{f}^{b}-\left(2\hat{\boldsymbol{\omega}}_{ie}^{n}+\hat{\boldsymbol{\omega}}_{en}^{n}\right)\times\delta\boldsymbol{v}^{n}-\left(2\delta\boldsymbol{\omega}_{ie}^{n}+\delta\boldsymbol{\omega}_{en}^{n}\right)\times\boldsymbol{v}^{n} \end{cases} \tag{1}$$

where $\boldsymbol{\phi}=(\phi_E,\phi_N,\phi_U)$ and $\delta\mathbf{v}^n=(\delta v_E,\delta v_N,\delta v_U)$are the attitude error and velocity error in *n*-frame; $\mathbf{v}^n=(v_E,v_N,v_U)$ is the velocity of the vehicle; $\boldsymbol{C}_{\omega}^{-1}$is a relation matrix which transform the relative angular velocity between n'-frame and *n*-frame into the Euler angle error; $\boldsymbol{C}_{n}^{n'}$, $\boldsymbol{C}_{b}^{n'}$ and $\boldsymbol{C}_{b}^{n}$ are the rotation matrices; $\hat{\boldsymbol{f}}^{b}$ is the measured specific force in the *b*-frame, whose error $\delta\boldsymbol{f}^{b}$ consists of the accelerometer zero-bias ∇^b and white noise $\boldsymbol{\omega}_{a}^{b}$; $\delta\boldsymbol{\omega}_{ib}^{b}$ is the measurement error of the gyro, which is composed of constant drift $\boldsymbol{\varepsilon}^b$ and white noise $\boldsymbol{\omega}_{g}^{b}$; $\boldsymbol{\omega}_{ie}^{n}$ is the rotational angular velocity of the earth; $\boldsymbol{\omega}_{en}^{n}$ is the angular velocity of the vehicle relative to the earth; $\boldsymbol{\omega}_{in}^{n}=\boldsymbol{\omega}_{ie}^{n}+\boldsymbol{\omega}_{en}^{n}$ is the relative angular velocity between the *n*-frame and *i*-frame; and $\hat{\boldsymbol{\omega}}_{ie}^{n}$, $\hat{\boldsymbol{\omega}}_{en}^{n}$ and $\hat{\boldsymbol{\omega}}_{in}^{n}$ are the actual values of $\boldsymbol{\omega}_{ie}^{n}$, $\boldsymbol{\omega}_{en}^{n}$, $\boldsymbol{\omega}_{in}^{n}$ in the n'-frame, where $\delta\boldsymbol{\omega}_{ie}^{n}$, $\delta\boldsymbol{\omega}_{en}^{n}$ and $\delta\boldsymbol{\omega}_{in}^{n}$ represent the corresponding errors.

The position error equation of INS is given as [5,6]

$$\begin{cases} \delta\dot{L} = \dfrac{\delta v_N}{R_M+h}-\delta h\dfrac{v_N}{(R_M+h)^2} \\ \delta\dot{\lambda} = \dfrac{\delta v_E\sec L}{R_N+h}+\delta L\dfrac{v_E\tan L\sec L}{R_N+h}-\delta h\dfrac{v_E\sec L}{(R_N+h)^2} \\ \delta\dot{h} = \delta v_U \end{cases} \tag{2}$$

where $\delta\boldsymbol{p}=(\delta L,\delta\lambda,\delta h)$ is the position error in *n*-frame; *L* and *h* represent the latitude and altitude of the vehicle; and R_M and R_N are the median radius and normal radius.

In the general case, the gyro constant drift $\boldsymbol{\varepsilon}^b$ and accelerometer zero-bias ∇^b are described by random constants [5,28], i.e.

$$\dot{\boldsymbol{\varepsilon}}_{i}^{b}=0\ \ (i=x,y,z) \tag{3}$$

$$\dot{\nabla}_{i}^{b}=0\ \ (i=x,y,z) \tag{4}$$

Define the system state vector as

$$\boldsymbol{x}(t) = \left[\boldsymbol{\phi}, \delta\boldsymbol{v}^n, \delta\boldsymbol{p}, \boldsymbol{\varepsilon}^b, \nabla^b\right]^{\mathrm{T}} \tag{5}$$

The process model of the INS/GPS integration system can be established by combining (1)-(4) according to the selected system state, which follows

$$\dot{\boldsymbol{x}}(t) = \bar{f}(\boldsymbol{x}(t)) + \boldsymbol{w}(t) \tag{6}$$

where $\bar{f}(\cdot)$ is a nonlinear function describing the dynamics of the system state in continuous form, and $\boldsymbol{w}(t) = [(-\boldsymbol{C}_{\omega}^{-1}\boldsymbol{C}_b^{n'}\boldsymbol{\omega}_a^b)^T, (\boldsymbol{C}_b^n\boldsymbol{\omega}_g^b)^T, \boldsymbol{0}_{1\times 9}]^T$ is the process noise vector.

Applying the improved Euler discretization formulation [35] to discretize (6), the discrete-time process model for INS/GPS integration can be further obtained by

$$\boldsymbol{x}_k = f(\boldsymbol{x}_{k-1}) + \boldsymbol{w}_k \tag{7}$$

Remark 1. Supposing the step size for discretization is h, (7) is actually obtained from its continuous form by using the improved Euler discretization formulation $f(\boldsymbol{x}_{k-1}) = \boldsymbol{x}_{k-1} + h/2\{\bar{f}(\boldsymbol{x}_{k-1}) + \bar{f}(\boldsymbol{x}_{k-1} + h\cdot\bar{f}(\boldsymbol{x}_{k-1}))\}$.

2.2. Measurement model

The difference between INS and GPS in terms of velocity and position is taken as the measurement vector, i.e.

$$\boldsymbol{z}_k = [\,v_E - v_{EG} \quad v_N - v_{NG} \quad v_U - v_{UG} \quad L_I - L_G \quad \lambda_I - \lambda_G \quad h_I - h_G\,]^T \tag{8}$$

where $(v_E, v_N, v_U)^T$ and $(L, \lambda, h)^T$ are the velocity and position output by INS; $(v_{EG}, v_{NG}, v_{UG})^T$ and $(L_G, \lambda_G, h_G)^T$ are the velocity and position achieved by GPS.

Then, the measurement model for the INS/GPS integrated navigation system can be constructed as

$$\boldsymbol{z}_k = \begin{bmatrix}\mathbf{H}_v \\ \mathbf{H}_p\end{bmatrix}\boldsymbol{x}_k + \begin{bmatrix}\boldsymbol{v}_{vk} \\ \boldsymbol{v}_{pk}\end{bmatrix} = \mathbf{H}_k\boldsymbol{x}_k + \boldsymbol{v}_k \tag{9}$$

where $\mathbf{H}_v = [\boldsymbol{0}_{3\times 3}, \boldsymbol{I}_{3\times 3}, \boldsymbol{0}_{3\times 9}]$, $\mathbf{H}_p = [\boldsymbol{0}_{3\times 6}, diag(R_M,\ R_N\cos L,\ 1), \boldsymbol{0}_{3\times 6}]$; $\boldsymbol{v}_{vk}$ and $\boldsymbol{v}_{pk}$ are the measurement noises, which correspond to the velocity and position errors of GPS, respectively.

3. Maximum likelihood based adaptive unscented kalman filter

This section develops a new MLAUKF with process noise covariance estimation to prevent the performance degradation of the standard UKF due to process noise uncertainty. The proposed MLAUKF constructs the conditional probability density of measurement using the statistical information of innovation vector. Afterwards, it estimates process noise covariance based on the ML principle, in which an estimation window for fixed-length memory is introduced to emphasize the use of the new observations. The obtained estimation is eventually fed back to the adaptive filtering process to adjust the Kalman gain matrix.

3.1. Standard ukf

To facilitate the derivation of the MLAUKF, the concept of the standard UKF is briefly reviewed at first. Consider the nonlinear discrete-time system consisting of (7) and (9)

$$\begin{cases}\boldsymbol{x}_k = f(\boldsymbol{x}_{k-1}) + \boldsymbol{w}_k \\ \boldsymbol{z}_k = \mathbf{H}_k\boldsymbol{x}_k + \boldsymbol{v}_k\end{cases} \tag{10}$$

where $\boldsymbol{x}_k \in \mathbf{R}^n$ and $\boldsymbol{z}_k \in \mathbf{R}^m$ denote the state of dynamic system and its corresponding noisy measurement at time point k; $\boldsymbol{w}_k$ and $\boldsymbol{v}_k$ are uncorrelated zero-mean Gaussian white noises with covariances $E[\boldsymbol{w}_k\boldsymbol{w}_k^T] = \mathbf{Q}$ and $E[\boldsymbol{v}_k\boldsymbol{v}_k^T] = \mathbf{R}$; and $f(\cdot)$ is the nonlinear function describing the process model and $\mathbf{H}_k$ is the measurement matrix.

The computational process of the standard UKF for the nonlinear system described by (10) involves the following steps:

Step 1. Assume state estimate $\hat{\boldsymbol{x}}_{k-1}$ and its error covariance matrix $\hat{\mathbf{P}}_{k-1}$ are given. The sigma points can be selected as

$$\begin{cases}\boldsymbol{\xi}_{i,k-1} = \hat{\boldsymbol{x}}_{k-1}\, i = 0 \\ \boldsymbol{\xi}_{i,k-1} = \hat{\boldsymbol{x}}_{k-1} + a\left(\sqrt{n\hat{\mathbf{P}}_{k-1}}\right)_i \quad i = 1, 2, \cdots, n \\ \boldsymbol{\xi}_{i,k-1} = \hat{\boldsymbol{x}}_{k-1} - a\left(\sqrt{n\hat{\mathbf{P}}_{k-1}}\right)_{i-n} \quad i = n+1, n+2, \cdots, 2n\end{cases} \tag{11}$$

where a is the tuning parameter which describes the spread of the sigma points around $\hat{\boldsymbol{x}}_{k-1}$, and $(\sqrt{n\hat{\mathbf{P}}_{k-1}})_i$is the ith column of $\sqrt{n\hat{\mathbf{P}}_{k-1}}$.

Step 2. Prediction: Each of the sigma points is transformed through the process model to yield a new set of samples

$$\boldsymbol{\xi}_{i,k/k-1} = f\left(\boldsymbol{\xi}_{i,k-1}\right) \quad (i = 0, 1, \cdots, 2n) \tag{12}$$

The predicted mean and covariance are calculated as

$$\hat{\boldsymbol{x}}_{k/k-1} = \sum_{i=0}^{2n}\omega_i\boldsymbol{\xi}_{i,k/k-1} \tag{13}$$

$$\hat{\mathbf{P}}_{k/k-1} = \sum_{i=0}^{2n}\omega_i\left(\boldsymbol{\xi}_{i,k/k-1} - \hat{\boldsymbol{x}}_{k/k-1}\right)\left(\boldsymbol{\xi}_{i,k/k-1} - \hat{\boldsymbol{x}}_{k/k-1}\right)^T + \mathbf{Q} \tag{14}$$

where $\begin{cases}\omega_i = 1 - \dfrac{1}{a^2}\, i = 0 \\ \omega_i = \dfrac{1}{2na^2}\, i = 1, 2, \cdots, 2n\end{cases}$.

Step 3. Update: Since the measurement model is with linear characteristic, the update process can be performed in the same way as the Kalman filter.

$$\hat{\boldsymbol{z}}_{k/k-1} = \mathbf{H}_k\hat{\boldsymbol{x}}_{k/k-1} \tag{15}$$

$$\hat{\mathbf{P}}_{\boldsymbol{z}_{k/k-1}} = \mathbf{H}_k\hat{\mathbf{P}}_{k/k-1}\mathbf{H}_k^T + \mathbf{R} \tag{16}$$

$$\hat{\mathbf{P}}_{\hat{\boldsymbol{x}}_{k/k-1}\hat{\boldsymbol{z}}_{k/k-1}} = \hat{\mathbf{P}}_{k/k-1}\mathbf{H}_k^T \tag{17}$$

$$\mathbf{K}_k = \hat{\mathbf{P}}_{\hat{\boldsymbol{x}}_{k/k-1}\hat{\boldsymbol{z}}_{k/k-1}}\hat{\mathbf{P}}_{\boldsymbol{z}_{k/k-1}}^{-1} \tag{18}$$

$$\hat{\boldsymbol{x}}_k = \hat{\boldsymbol{x}}_{k/k-1} + \mathbf{K}_k\left(\boldsymbol{z}_k - \hat{\boldsymbol{z}}_{k/k-1}\right) \tag{19}$$

$$\hat{\mathbf{P}}_k = \hat{\mathbf{P}}_{k/k-1} - \mathbf{K}_k\hat{\mathbf{P}}_{\boldsymbol{z}_{k/k-1}}\mathbf{K}_k^T \tag{20}$$

Step 4. Go to Step 1 for the next sample until all samples are processed.

3.2. Estimation of process noise covariance

Denote the innovation vector by

$$\tilde{\boldsymbol{z}}_k = \boldsymbol{z}_k - \hat{\boldsymbol{z}}_{k/k-1} \tag{21}$$

It is apparent that the covariance of the innovation vector is $\hat{\mathbf{P}}_{\boldsymbol{z}_{k/k-1}}$ given by (16), and the conditional probability density of the measurement vector $\boldsymbol{z}_k$ can be described as

$$p_{(\boldsymbol{z}|\mathbf{Q})_k} = \frac{1}{\sqrt{(2\pi)^m\left|\hat{\mathbf{P}}_{\boldsymbol{z}_{k/k-1}}\right|}}\exp\left(-\frac{1}{2}\tilde{\boldsymbol{z}}_k^{\mathrm{T}}\hat{\mathbf{P}}_{\boldsymbol{z}_{k/k-1}}^{-1}\tilde{\boldsymbol{z}}_k\right) \tag{22}$$

where m is the dimension of the measurement vector, and $|\cdot|$ is the determinant operator.

Using algebraic manipulation, the likelihood function of the mea-

surement $(z_{k-N+1}, z_{k-N+2}, \cdots, z_k)$ can be obtained as

$$L(\mathbf{Q}|z_{k-N+1:k}) = \prod_{j=k-N+1}^{k} p_{(z|\mathbf{Q})_j} = \prod_{j=k-N+1}^{k} \frac{1}{\sqrt{(2\pi)^m \left|\hat{\mathbf{P}}_{\tilde{z}_{j/j-1}}\right|}} \exp\left(-\frac{1}{2}\tilde{z}_j^{\mathrm{T}} \hat{\mathbf{P}}_{\tilde{z}_{j/j-1}}^{-1} \tilde{z}_j\right) \tag{23}$$

where N is the window size for fixed-length memory.

Thus, based on the ML principle, the parameter $\mathbf{Q}$ can be estimated by

$$\hat{\mathbf{Q}}_{ML} = \arg\max_{\mathbf{Q}} \{L(\mathbf{Q}|z_{k-N+1:k})\} \tag{24}$$

Taking the natural logarithm of (23) yields

$$\ln L(\mathbf{Q}|z_{k-N+1:k}) = -\frac{1}{2} \sum_{j=k-N+1}^{k} \left\{ ln(|\hat{\mathbf{P}}_{\tilde{z}_{j/j-1}}|) + \tilde{z}_j^{\mathrm{T}} \hat{\mathbf{P}}_{\tilde{z}_{j/j-1}}^{-1} \tilde{z}_j \right\} + const \tag{25}$$

Multiplying (25) by -2 and neglecting the constant term, it is further derived that the ML estimation of $\mathbf{Q}$ fulfills the following condition

$$\hat{\mathbf{Q}}_{ML} = \arg\min_{\mathbf{Q}} \left[\sum_{j=k-N+1}^{k} \ln(|\hat{\mathbf{P}}_{\tilde{z}_{j/j-1}}|) + \sum_{j=k-N+1}^{k} \tilde{z}_j^{\mathrm{T}} \hat{\mathbf{P}}_{\tilde{z}_{j/j-1}}^{-1} \tilde{z}_j \right] \tag{26}$$

To resolve (26), a cost function is defined as

$$\boldsymbol{J}\left(\mathbf{Q}\right) = \sum_{j=k-N+1}^{k} \left\{ \ln(|\hat{\mathbf{P}}_{\tilde{z}_{j/j-1}}|) + \tilde{z}_j^{\mathrm{T}} \hat{\mathbf{P}}_{\tilde{z}_{j/j-1}}^{-1} \tilde{z}_j \right\} \tag{27}$$

Then, the ML equations are obtained by letting $\partial \boldsymbol{J} / \partial \mathbf{Q}_{il} = 0$, that is

$$\sum_{j=k-N+1}^{k} \left\{ tr\left[\hat{\mathbf{P}}_{\tilde{z}_{j/j-1}}^{-1} \frac{\partial \hat{\mathbf{P}}_{\tilde{z}_{j/j-1}}}{\partial \mathbf{Q}_{il}} \right] - \tilde{z}_j^{\mathrm{T}} \hat{\mathbf{P}}_{\tilde{z}_{j/j-1}}^{-1} \frac{\partial \hat{\mathbf{P}}_{\tilde{z}_{j/j-1}}}{\partial \mathbf{Q}_{il}} \hat{\mathbf{P}}_{\tilde{z}_{j/j-1}}^{-1} \tilde{z}_j \right\} = 0 \quad (i, l = 1, 2, \cdots, n) \tag{28}$$

where $tr\{\cdot\}$ represents the trace of a matrix, and $\mathbf{Q}_{il}(i, l = 1, 2, \cdots, n)$ is element of $\mathbf{Q}$ in the ith row and lth column.

Therefore, it can be seen from (28) that the problem to estimate process noise covariance $\mathbf{Q}$ is actually to calculate the derivative of innovation vector's covariance with respect to $\mathbf{Q}_{il}(i, l = 1, 2, \cdots, n)$.

Denote the state estimation error and prediction error as

$$\tilde{\boldsymbol{x}}_k = \boldsymbol{x}_k - \hat{\boldsymbol{x}}_k \tag{29}$$

$$\tilde{\boldsymbol{x}}_{k/k-1} = \boldsymbol{x}_k - \hat{\boldsymbol{x}}_{k/k-1} \tag{30}$$

Substituting (12) and (13) into (30) and expanding $f(\cdot)$ by a Taylor series about $\hat{\boldsymbol{x}}_{k-1}$ yield

$$\tilde{\boldsymbol{x}}_{k/k-1} = \mathbf{F}_k \tilde{\boldsymbol{x}}_{k-1} + \Delta(\tilde{\boldsymbol{x}}_{k-1}) + \boldsymbol{w}_k \tag{31}$$

where $\mathbf{F}_k = \frac{\partial f(\boldsymbol{x})}{\partial \boldsymbol{x}}|_{\boldsymbol{x}=\hat{\boldsymbol{x}}_{k-1}}$, and $\Delta(\tilde{\boldsymbol{x}}_{k-1})$ denotes the second and higher-order moments in the Taylor series.

In order to take into account all the estimation residuals to obtain an exact equality [18,35], we model the first-order linearization error in (31) by introducing an instrumental diagonal matrix $\boldsymbol{\beta}_k = diag(\beta_{1,k}, \beta_{2,k}, \cdots, \beta_{n,k})$. It is obtained that

$$\tilde{\boldsymbol{x}}_{k/k-1} = \boldsymbol{\beta}_k \mathbf{F}_k \tilde{\boldsymbol{x}}_{k-1} + \boldsymbol{w}_k \tag{32}$$

Thus, the predicted covariance $\hat{\mathbf{P}}_{k/k-1}$ can also be represented by

$$\begin{aligned} \hat{\mathbf{P}}_{k/k-1} &= E\left[\tilde{\boldsymbol{x}}_{k/k-1} \tilde{\boldsymbol{x}}^{\mathrm{T}}{}_{k/k-1}\right] \\ &= E\left[(\boldsymbol{\beta}_k \mathbf{F}_k \tilde{\boldsymbol{x}}_{k-1} + \boldsymbol{w}_k)(\boldsymbol{\beta}_k \mathbf{F}_k \tilde{\boldsymbol{x}}_{k-1} + \boldsymbol{w}_k)^{\mathrm{T}}\right] \\ &= \boldsymbol{\beta}_k \mathbf{F}_k \hat{\mathbf{P}}_{k-1} \mathbf{F}_k^{\mathrm{T}} \boldsymbol{\beta}_k + \mathbf{Q} \end{aligned} \tag{33}$$

Taking partial derivatives of (16) and (33) with respect to $\mathbf{Q}_{il}$ yields

$$\frac{\partial \hat{\mathbf{P}}_{\tilde{z}_{k/k-1}}}{\partial \mathbf{Q}_{il}} = \frac{\partial \mathbf{R}}{\partial \mathbf{Q}_{il}} + \mathbf{H}_k \frac{\partial \hat{\mathbf{P}}_{k/k-1}}{\partial \mathbf{Q}_{il}} \mathbf{H}_k^T \tag{34}$$

and

$$\frac{\partial \hat{\mathbf{P}}_{k/k-1}}{\partial \mathbf{Q}_{il}} = \boldsymbol{\beta}_k \mathbf{F}_k \frac{\partial \hat{\mathbf{P}}_{k-1}}{\partial \mathbf{Q}_{il}} \mathbf{F}_k^{\mathrm{T}} \boldsymbol{\beta}_k + \frac{\partial \mathbf{Q}}{\partial \mathbf{Q}_{il}} \tag{35}$$

It has been shown in [31,32] that, as the filtering process inside the estimation window reaches the steady state, the first term on the right side of (35) can be neglected. Thus, substituting (35) into (34) and considering $\frac{\partial \mathbf{R}}{\partial \mathbf{Q}_{il}} = \mathbf{0}$, it is achieved

$$\frac{\partial \hat{\mathbf{P}}_{\tilde{z}_{k/k-1}}}{\partial \mathbf{Q}_{il}} = \mathbf{H}_k \frac{\partial \mathbf{Q}}{\partial \mathbf{Q}_{il}} \mathbf{H}_k^T \tag{36}$$

Then, substituting (36) into (28) and rearranging it, the ML Eq. (28) becomes

$$\sum_{j=k-N+1}^{k} tr\left\{ \mathbf{H}_j^T \cdot \left[\hat{\mathbf{P}}_{\tilde{z}_{j/j-1}}^{-1} - \hat{\mathbf{P}}_{\tilde{z}_{j/j-1}}^{-1} \tilde{z}_j \tilde{z}_j^{\mathrm{T}} \hat{\mathbf{P}}_{\tilde{z}_{j/j-1}}^{-1} \right] \cdot \mathbf{H}_j \cdot \frac{\partial \mathbf{Q}}{\partial \mathbf{Q}_{il}} \right\} = 0 \quad (i, l = 1, 2, \cdots, n) \tag{37}$$

which can be further rewritten as

$$\sum_{j=k-N+1}^{k} \left\{ \mathbf{H}_j^T \cdot \left[\hat{\mathbf{P}}_{\tilde{z}_{j/j-1}}^{-1} - \hat{\mathbf{P}}_{\tilde{z}_{j/j-1}}^{-1} \tilde{z}_j \tilde{z}_j^{\mathrm{T}} \hat{\mathbf{P}}_{\tilde{z}_{j/j-1}}^{-1} \right] \cdot \mathbf{H}_j \right\}_{li} = 0 \quad (i, l = 1, 2, \cdots, n) \tag{38}$$

Sequentially, inserting (17) into (18), the Kalman gain $\mathbf{K}_k$ is derived as

$$\mathbf{K}_k = \hat{\mathbf{P}}_{k/k-1} \mathbf{H}_k^T \hat{\mathbf{P}}_{\tilde{z}_{k/k-1}}^{-1} \tag{39}$$

Eq. (39) can also be equivalently expressed as

$$\mathbf{H}_k^T \hat{\mathbf{P}}_{\tilde{z}_{k/k-1}}^{-1} = \hat{\mathbf{P}}_{k/k-1}^{-1} \mathbf{K}_k \tag{40}$$

and

$$\hat{\mathbf{P}}_{\tilde{z}_{k/k-1}}^{-1} \mathbf{H}_k = \mathbf{K}_k^T \hat{\mathbf{P}}_{k/k-1}^{-1} \tag{41}$$

Substituting (40) and (41) into (38) and rearranging it, we have

$$\sum_{j=k-N+1}^{k} \left\{ \hat{\mathbf{P}}_{j/j-1}^{-1} \left[\mathbf{K}_j \mathbf{H}_j \hat{\mathbf{P}}_{j/j-1} - \mathbf{K}_j \tilde{z}_j \tilde{z}_j^{\mathrm{T}} \mathbf{K}_j^{\mathrm{T}} \right] \hat{\mathbf{P}}_{j/j-1}^{-1} \right\}_{li} = 0 \quad (i, l = 1, 2, \cdots, n) \tag{42}$$

From (33), which is equivalent to (14), it is easy to find that $\hat{\mathbf{P}}_{k/k-1}^{-1}$ is a function of $\mathbf{Q}$. However, in general, it is still not possible to achieve a closed form solution for $\mathbf{Q}$ based on the above Eq. (42). In the following, by assuming the filter works in the steady state [32], an explicitly approximate estimator for $\mathbf{Q}$ is obtained. The asymptotic unbiasedness and convergence of this estimator is further proved in Section 3.4.

Assume the filtering process inside the estimation window is in steady state such that $\hat{\mathbf{P}}_{j/j-1}$ are approximately constant for all j ($j = k - N + 1, k - N + 2, \cdots, k$). Then, (42) becomes

$$\left\{ \hat{\mathbf{P}}_{k/k-1}^{-1} \cdot \sum_{j=k-N+1}^{k} \left[\mathbf{K}_j \mathbf{H}_j \hat{\mathbf{P}}_{j/j-1} - \mathbf{K}_j \tilde{z}_j \tilde{z}_j^{\mathrm{T}} \mathbf{K}_j^{\mathrm{T}} \right] \cdot \hat{\mathbf{P}}_{k/k-1}^{-1} \right\}_{li} = 0 \quad (i, l = 1, 2, \cdots, n) \tag{43}$$

and the above Eq. (43) is satisfied if

$$\sum_{j=k-N+1}^{k} \left[\mathbf{K}_j \mathbf{H}_j \hat{\mathbf{P}}_{j/j-1} - \mathbf{K}_j \tilde{z}_j \tilde{z}_j^{\mathrm{T}} \mathbf{K}_j^{\mathrm{T}} \right] = \mathbf{0} \tag{44}$$

Besides, it is known from the UKF procedure described in (10)-(20) that

$$\mathbf{K}_k\tilde{z}_k=\hat{\boldsymbol{x}}_k-\hat{\boldsymbol{x}}_{k/k-1} \tag{45}$$

$$\hat{\mathbf{P}}_{k/k-1}-\hat{\mathbf{P}}_k=\mathbf{K}_k\mathbf{H}_k\hat{\mathbf{P}}_{k/k-1} \tag{46}$$

Substituting (14), (45) and (46) into (44), the ML estimate of process noise covariance $\mathbf{Q}$ can be obtained as

$$\hat{\mathbf{Q}}_{ML}=\frac{1}{N}\sum_{j=k-N+1}^{k}\left[\begin{array}{l}\hat{\mathbf{P}}_j+\left(\hat{\boldsymbol{x}}_j-\hat{\boldsymbol{x}}_{j/j-1}\right)\left(\hat{\boldsymbol{x}}_j-\hat{\boldsymbol{x}}_{j/j-1}\right)^T\\-\sum_{i=0}^{2n}\omega_i\left(\boldsymbol{\xi}_{i,j/j-1}-\hat{\boldsymbol{x}}_{j/j-1}\right)\left(\boldsymbol{\xi}_{i,j/j-1}-\hat{\boldsymbol{x}}_{j/j-1}\right)^T\end{array}\right] \tag{47}$$

Remark 2. Since (42) is a nonlinear equation, an iterative method is generally employed to find the optimal solution for $\mathbf{Q}$. For example, the Newton-Raphson iteration can be used:

$$\hat{\mathbf{Q}}_{il}(L+1)=\hat{\mathbf{Q}}_{il}(L)+\left(\frac{\partial^2\boldsymbol{J}}{\partial^2\mathbf{Q}_{il}}\right)^{-1}\frac{\partial\boldsymbol{J}}{\partial\mathbf{Q}_{il}}\bigg|_{\hat{\mathbf{Q}}_{il}(L)} \tag{48}$$

where $\partial\boldsymbol{J}/\partial\mathbf{Q}_{il}$ is the left side of (42), L denotes the iteration number, and $\mathbf{Q}_{il}$ denotes the element of $\mathbf{Q}$ in the ith row and lth column.

However, on the other hand, because too many calculations of partial derivatives are required, the above iterative solution is commonly applied to data post-processing rather than real-time estimation, even though it is optimal in the sense of numerical computation.

Remark 3. As conducted in various INS based applications such as [9,31,36], the process noise covariance $\mathbf{Q}$, which characterizes the covariance of the white noise involved in the inertial sensors, is usually set as a positive diagonal matrix. Under this condition, the estimation of $\mathbf{Q}$ is simplified as the estimation of the diagonal elements of $\mathbf{Q}$, and the ML estimator can be presented as

$$\hat{\mathbf{Q}}_{ML}=\frac{1}{N}\sum_{j=k-N+1}^{k}\left[\begin{array}{l}diag\left(\left(\hat{\mathbf{P}}_j\right)_{11},\left(\hat{\mathbf{P}}_j\right)_{22},\ldots,\left(\hat{\mathbf{P}}_j\right)_{nn}\right)+\left(\hat{\boldsymbol{x}}_j-\hat{\boldsymbol{x}}_{j/j-1}\right)\left(\hat{\boldsymbol{x}}_j-\hat{\boldsymbol{x}}_{j/j-1}\right)^T\\-\sum_{i=0}^{2n}\omega_i\left(\boldsymbol{\xi}_{i,j/j-1}-\hat{\boldsymbol{x}}_{j/j-1}\right)\left(\boldsymbol{\xi}_{i,j/j-1}-\hat{\boldsymbol{x}}_{j/j-1}\right)^T\end{array}\right] \tag{49}$$

3.3. MLAUKF algorithm

The hypothesis testing theory can be used to identify whether the filtering process inside the estimation window reaches the steady state, aiming to update the process noise covariance $\mathbf{Q}$ with higher accuracy by the ML estimator.

Denote the innovation vector by $\tilde{z}_k=z_k-\hat{z}_{k/k-1}$ and its theoretical covariance by $\sigma^2=\hat{\mathbf{P}}_{\tilde{z}_{k/k-1}}=\mathbf{H}_k\hat{\mathbf{P}}_{k/k-1}\mathbf{H}_k^T+\mathbf{R}$. As the filter works in steady state, 95.45% value of $\tilde{z}_k$ will fall in the scope around zero mean within a range of 2σ [5]. Thus, the procedure for hypothesis testing can be briefly described as:

Null hypothesis γ_0: the filtering process is in the steady state;

Alternative hypothesis γ_1: the filtering process is not in the steady state. where the null hypothesis γ_0 is fulfilled if $\tilde{z}_k$ falls in the scope around zero mean within a range of 2σ; and otherwise, the alternative hypothesis γ_1 is fulfilled.

Base on the above analysis and combining the ML estimator (47) or (49) with the standard UKF, the MLAUKF process can be summarized as follow:

Step 1. Assume that the state estimate $\hat{\boldsymbol{x}}_{k-1}$ and the error covariance matrix $\hat{\mathbf{P}}_{k-1}$ for the time point $k-1$ are given;

Step 2. Execute the standard UKF as usual by following (11) to (20);

Step 3. Update the process noise covariance;

Identify whether the filtering process is in the steady state. If yes, do the following two operations:

- Update the estimate of process noise covariance $\hat{\mathbf{Q}}_{ML}$ by (47) or (49);
- Reset $\mathbf{Q}=\hat{\mathbf{Q}}_{ML}$ and go to **Step 1.**

Otherwise, return to **Step 1** directly.

Step 4. Repeat **Steps 1** to **3** for the next sample until all samples are processed.

Remark 4 Based on the computational cost analysis of UKF in our previous work [2], we can readily obtain that the total computational cost expended by UKF is $31/3n^3+m^3+6m^2n+4mn^2+19n^2+4mn+m^2+m+5n$ flop counts and $2n+1$ dynamic nonlinear mappings per update cycle for the nonlinear system (10). Note that except for the estimation procedure of process noise covariance $\mathbf{Q}$, the flops involved in the other steps are the same for both UKF and MLAUKF. Thus, considering the computational cost involved in (47) which is $2n^3+7n^2+4n$ with iterative method, it is achieved that the computational load of MLAUKF is $37/3n^3+m^3+6m^2n+4mn^2+26n^2+4mn+m^2+m+9n$ flops and$2n+1$ dynamic nonlinear mappings per update cycle.

Remark 5. If the ML estimator (49) is adopted to estimate $\mathbf{Q}$, the computational load of the MLAUKF will reduce to $37/3n^3+m^3+6m^2n+4mn^2+25n^2+4mn+m^2+m+10n$ flop counts and $2n+1$ dynamic nonlinear mappings per update cycle. This is because the computational cost of (49), which is $2n^3+6n^2+5n$ flops, is less than that of (47). Nevertheless, it is also clear that the computational load of MLAUKF based on either the ML estimator (47) or (49) is slightly larger than that of UKF.

3.4. Discussion on mlaukf

The asymptotic convergence and unbiasedness of the ML estimator (47) as well as the stochastic stability of the proposed MLAUKF is discussed below.

Theorem 1. *Suppose the filtering process inside the estimation window for fixed-length memory is in the steady state, then the ML estimator (47) converges to* $\mathbf{Q}$ *in probability as the window size* $N\to\infty$.

Proof With the assumption that the filtering process is in the steady state, it can be seen from the derivation of (47) that the ML estimator is actually the optimal solution to (42). Thus, the asymptotic convergence of the obtained ML estimator can be proved identically to that of the ML estimation of noise statistics in linear systems as shown in [32].

Theorem 2. *Suppose the estimation window size for fixed-length memory is N and the process noise covariance is constant or have small variations in this window. Then the ML estimator (47) is unbiased.*

Proof Taking the expectation of (47) gives

where Eqs. (14), (20) and (45) are used. The proof of Theorem 2 is completed.

$$
\begin{aligned}
E\left[\hat{\mathbf{Q}}_{ML}\right] &= \frac{1}{N}\sum_{j=k-N+1}^{k} E\left[\hat{\mathbf{P}}_j + \left(\hat{\boldsymbol{x}}_j - \hat{\boldsymbol{x}}_{j/j-1}\right)\left(\hat{\boldsymbol{x}}_j - \hat{\boldsymbol{x}}_{j/j-1}\right)^T - \sum_{i=0}^{2n}\omega_i\left(\boldsymbol{\xi}_{i,j/j-1} - \hat{\boldsymbol{x}}_{j/j-1}\right)\left(\boldsymbol{\xi}_{i,j/j-1} - \hat{\boldsymbol{x}}_{j/j-1}\right)^T\right] \\
&= \frac{1}{N}\sum_{j=k-N+1}^{k}\left[\hat{\mathbf{P}}_j + \mathbf{K}_j \cdot E\left(\tilde{z}_j\tilde{z}_j^{\mathrm{T}}\right)\cdot\mathbf{K}_j^{\mathrm{T}} - \left(\hat{\mathbf{P}}_{j/j-1} - \mathbf{Q}\right)\right] \\
&= \frac{1}{N}\sum_{j=k-N+1}^{k}\left[\hat{\mathbf{P}}_j - \left(\hat{\mathbf{P}}_{j/j-1} - \mathbf{K}_j\hat{\mathbf{P}}_{z_{k/k-1}}\mathbf{K}_j^{\mathrm{T}}\right) + \mathbf{Q}\right] \\
&= \mathbf{Q}
\end{aligned}
\tag{50}
$$

Assume the estimation window size in the ML estimator is N. From Theorem 1, it is verified that there exists an error matrix $\delta\mathbf{Q}$ such that the following equations hold:

$$
\lim_{N\to\infty}\delta\mathbf{Q} = \mathbf{0} \tag{51}
$$

$$
\hat{\mathbf{Q}}_{ML} = \mathbf{Q} + \delta\mathbf{Q} \tag{52}
$$

Thus, similar to (33), the predicted covariance in the proposed MLAUKF can be rewritten as

$$
\begin{aligned}
\hat{\mathbf{P}}_{k/k-1} &= \boldsymbol{\beta}_k\mathbf{F}_k\hat{\mathbf{P}}_{k-1}\mathbf{F}_k^{\mathrm{T}}\boldsymbol{\beta}_k + \hat{\mathbf{Q}}_{ML} \\
&= \boldsymbol{\beta}_k\mathbf{F}_k\hat{\mathbf{P}}_{k-1}\mathbf{F}_k^{\mathrm{T}}\boldsymbol{\beta}_k + \mathbf{Q} + \delta\mathbf{Q}
\end{aligned}
\tag{53}
$$

We make a slight modification to (53) by adding an extra positive definite matrix $\Delta\mathbf{Q}$, such that

$$
\begin{aligned}
\hat{\mathbf{P}}_{k/k-1} &= \boldsymbol{\beta}_k\mathbf{F}_k\hat{\mathbf{P}}_{k-1}\mathbf{F}_k^{\mathrm{T}}\boldsymbol{\beta}_k + \hat{\mathbf{Q}}_{ML} \\
&= \boldsymbol{\beta}_k\mathbf{F}_k\hat{\mathbf{P}}_{k-1}\mathbf{F}_k^{\mathrm{T}}\boldsymbol{\beta}_k + \mathbf{Q} + \delta\mathbf{Q} + \Delta\mathbf{Q} \\
&= \boldsymbol{\beta}_k\mathbf{F}_k\hat{\mathbf{P}}_{k-1}\mathbf{F}_k^{\mathrm{T}}\boldsymbol{\beta}_k + \hat{\mathbf{Q}}_{sum}
\end{aligned}
\tag{54}
$$

where $\hat{\mathbf{Q}}_{sum} = \mathbf{Q} + \delta\mathbf{Q} + \Delta\mathbf{Q}$.

Thus, the stochastic stability of the proposed MLAUKF can be ensured under the sufficient conditions presented in Theorem 3.

Theorem 3. *Consider the nonlinear stochastic systems given by (10) and the MLAUKF described by (11)-(13), (54) and (15)-(20), in which the process noise covariance is updated by (47) or (49). Let the following assumptions hold for every $k \geq 0$:*

(1) There exist real constants $f_{\min}$, $f_{\max}$, $h_{\min}$, $h_{\max}$, $c_{\min} \neq 0$, $c_{\max} \neq 0$ such that the following bounds are fulfilled:

$$
f_{\min}^2 \leq \mathbf{F}_k\mathbf{F}_k^T \leq f_{\max}^2,\ \ h_{\min}^2 \leq \mathbf{H}_k\mathbf{H}_k^T \leq h_{\max}^2,\ \ c_{\min}^2\mathbf{I} \leq \boldsymbol{\beta}_k\boldsymbol{\beta}_k^T \leq c_{\max}^2\mathbf{I} \tag{55}
$$

where $\mathbf{F}_k$ presents the first-order derivative of the nonlinear function$f(\cdot)$ as in (31), and $\boldsymbol{\beta}_k$ is the introduced instrumental matrix in (53).

(1) There exist real constants $q_{\min}^*, q_{\max}^*, q_{\min}, q_{\max}, r_{\min}, p_{\min}, p_{\max} > 0$ such that the following bounds on matrices are fulfilled:

$$
\begin{aligned}
&q_{\min}\mathbf{I} \leq \mathbf{Q} \leq q_{\max}\mathbf{I},\ \ q_{\min}^*\mathbf{I} \leq \hat{\mathbf{Q}}_{sum} \leq q_{\max}^*\mathbf{I} \\
&\mathbf{R} \geq r_{min}\mathbf{I},\ \ p_{\min}\mathbf{I} \leq \hat{\mathbf{P}}_k \leq p_{\max}\mathbf{I}
\end{aligned}
\tag{56}
$$

Then, the MLAUKF estimation error $\tilde{x}_k$ defined in (29) is exponentially bounded in mean square.

Proof Taking the expression of the predicted covariance (54) into account, Theorem 3 can be directly derived by applying the results of Theorem 1 in [37]. Thus, the proof is omitted here for conciseness.

Remark 6. Since the ML estimator (49) is a special case of (47), it's asymptotic convergence and unbiasedness are ensured with the same conditions in Theorem 1 and Theorem 2, respectively.

Remark 7. The extra positive definite matrix $\Delta\mathbf{Q}$ actually plays a role for improvement of the MLAUKF's stability by satisfying $q_{\min}^*\mathbf{I} \leq \hat{\mathbf{Q}}_{sum} \leq q_{\max}^*\mathbf{I}$. This is also in agreement with the fact that the enlargement of the process noise covariance can improve the stability of UKF [35].

4. Performance evaluations and analysis

A prototype system of the vehicular INS/GPS integration was implemented using the proposed MLAUKF. The process and measurement models of this INS/GPS integration system are described by (7) and (9). Simulations and experiments as well as comparison analysis with UKF and adaptive robust UKF (ARUKF) [30] were conducted to comprehensively evaluate the performance of MLAUKF for the vehicular INS/GPS integrated navigation system. Further, given the fact that the process noise covariance in the vehicular INS/GPS integration is generally a diagonal matrix, the ML estimator (49) was employed in MLAUKF.

4.1. Simulations and analysis

Monte Carlo simulations were conducted to evaluate the performance of the proposed MLAUKF for vehicular INS/GPS integration. The designed vehicular trajectory is shown in Fig. 1, which involves various maneuvers such as linear motion with constant velocity, linear motion with constant acceleration and turning with variable acceleration. The initial position of the vehicle was at North latitude 34.246°, East longitude 108.997°, and altitude 500 m; the initial orientation was assumed to be parallel to the navigation frame; and the initial velocities along the three axes of the navigation frame E-N-U were 0 m/s, 10 m/s and 0 m/s, respectively. The initial position error was (10m, 10m, 15m), initial velocity error (0.3m/s, 0.3m/s, 0.3m/s) and initial attitude error (1′, 1′, 1.5′). The constant drift and white noise of the gyro were 0.1°/h and $0.01^\circ/\sqrt{\mathrm{h}}$. The bias and white noise of the accelerometer were $10^{-3}g$ and $10^{-4}g\cdot\sqrt{s}$. The root mean square errors (RMSEs) of GPS horizontal position, altitude and velocity were 3 m, 5 m and 0.05 m/s. The sampling periods of INS and GPS were 0.05 s and 1 s. The Monte Carlo simulations were carried out for 200 times with simulation time 1000s and filtering period of the INS/GPS integration 1 s. The estimation window size for fixed-length memory in MLAUKF was set as $N = 25$.

According to the aforementioned precision of the gyroscope and accelerometer, the real process noise covariance matrix for UKF, ARUKF and MLAUKF should be

$$
\mathbf{Q} = diag\left[\left(0.01^\circ/\sqrt{h}\right)^2\cdot\mathbf{I}_{3\times3}, \left(10^{-4}g\cdot\sqrt{s}\right)^2\cdot\mathbf{I}_{3\times3}, \mathbf{0}_{9\times9}\right] \tag{57}
$$

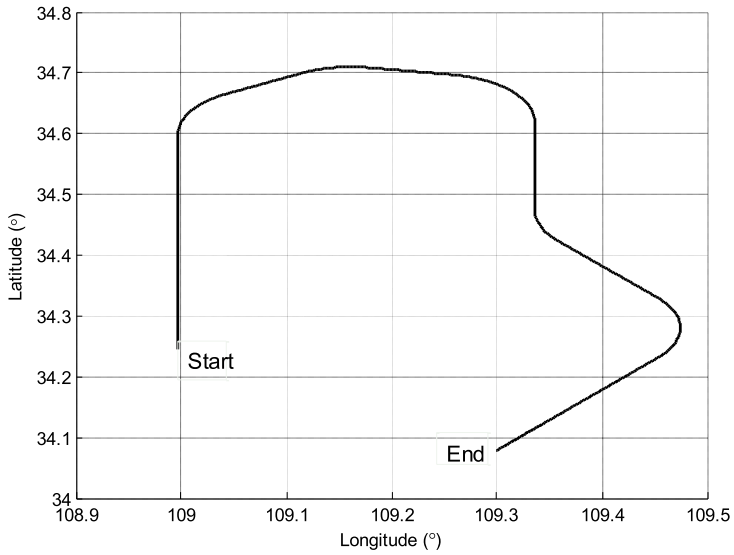

Fig. 1. Vehicular trajectory.

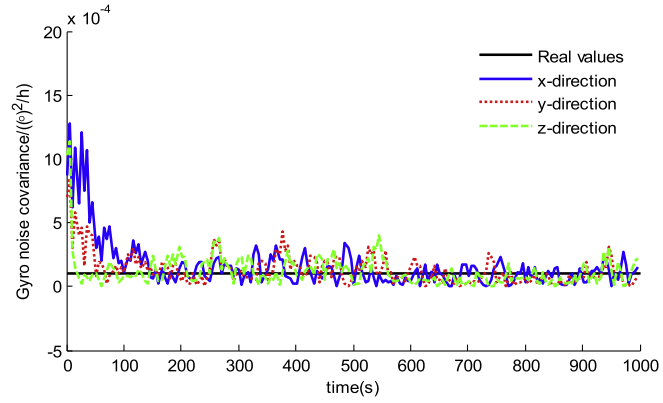

(a) Estimation of the gyro noise covariance

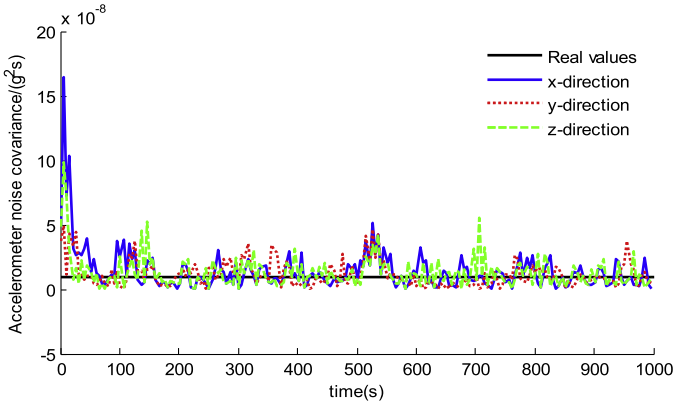

(b) Estimation of the accelerometer noise covariance

Fig. 2. Estimations of the noise covariances of gyro and accelerometer.

However, in order to evaluate the filtering performances of the above three methods in the presence of inaccurate process noise covariance, the initial process noise covariance actually adopted in the filters was set to 16*Q in the simulations.

The initial error covariance matrix was designed as the quadratic of the assumed initial state estimate error, and the covariance matrix of the measurement noise was designed according to the precision of GPS receiver. They are

$$\hat{\mathbf{P}}_0 = diag\Big[(1')^2, (1')^2, (1.5')^2, (0.3m/s)^2\mathbf{I}_{3\times3}, (10m)^2, (10m)^2, (15m)^2, (0.1^\circ/h)^2\mathbf{I}_{3\times3}, (10^{-3}g)^2\mathbf{I}_{3\times3}\Big] \tag{58}$$

$$\mathbf{R} = diag\Big[(0.05m/s)^2\mathbf{I}_{3\times3}, (3m)^2, (3m)^2, (5m)^2\Big] \tag{59}$$

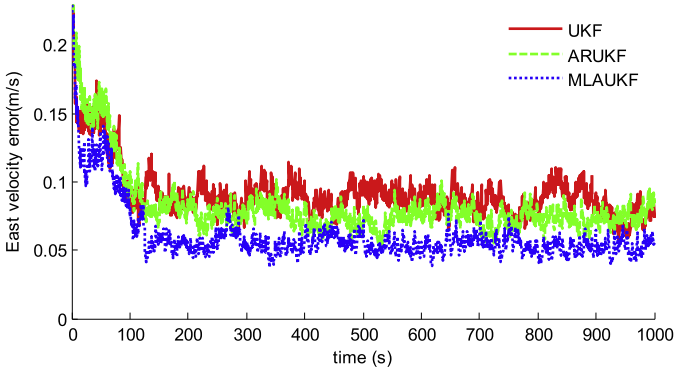

(a) RMSE of east velocity error

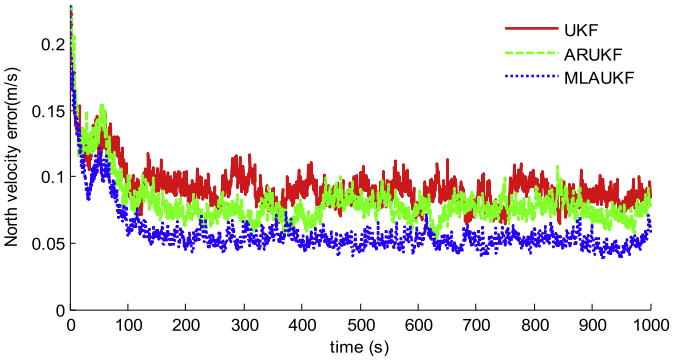

(b) RMSE of north velocity error

Fig. 3. RMSEs of the horizontal velocity errors obtained by UKF, ARUKF and MLAUKF.

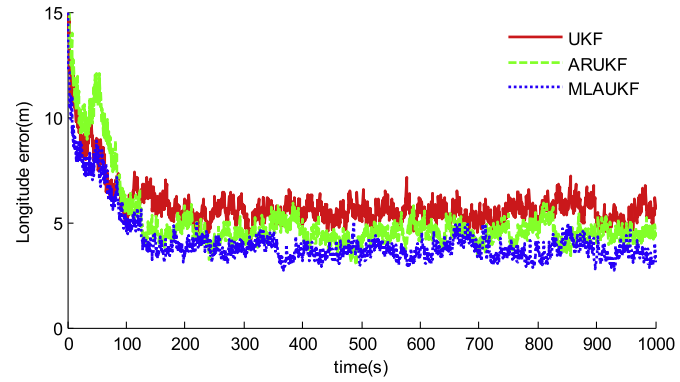

(a) RMSE of longitude error

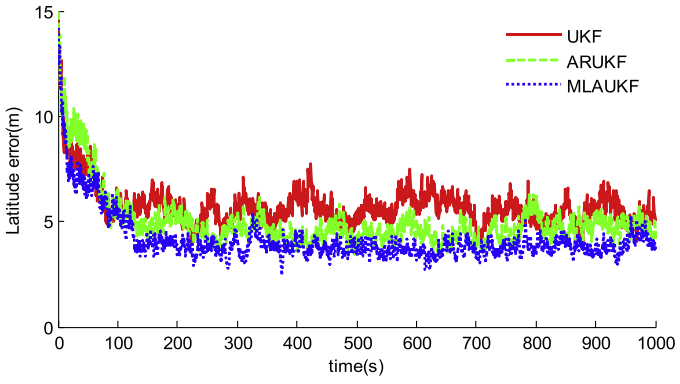

(b) RMSE of latitude error

Fig. 4. RMSEs of the horizontal position errors obtained by UKF, ARUKF and MLAUKF.

4.1.1. Estimation of process noise covariance

Trials were conducted to evaluate the performance of the proposed MLAUKF in terms of process noise covariance estimation. Fig. 2 shows the estimations of gyro and accelerometer noise covariances (i.e., the non-zero terms of the diagonal matrix **Q** in (57)) by MLAUKF. It can be seen from Fig. 2, the gyro and accelerometer noise covariances estimated by MLAUKF are very close to their real values after a short convergence procedure, even though the initial noise covariance matrix was enlarged to 16 times of the real one. During the time period from 100 s to 1000s, the estimation errors for gyro noise covariance are within $\pm 3.61 \times 10^{-4}(^0)^2/h$ and those for accelerometer noise covariance are within $\pm 4.03 \times 10^{-8} g^2 \cdot s$, respectively. The results demonstrate that the proposed MLAUKF can effectively estimate the process noise covariance and is promising to restrain the disturbance of process noise covariance's uncertainty on the filtering solution of UKF.

4.1.2. Navigation accuracy evaluation

Trials were further conducted to evaluate the performance of the proposed MLAUKF in terms of navigation accuracy. Figs. 3 and 4 depict the RMSEs of the horizontal velocity and position errors obtained by the three filters, from which we can observes the following:

i) Due to the disturbance of the incorrect process noise covariance, the UKF performance degrades seriously, resulting in the largest estimation errors in navigation solution.
ii) ARUKF slightly improves the UKF accuracy. This is because ARUKF incorporates the so-called adaptive factor and equivalent weight factor into the filtering process to weak the impact of system noise uncertainty on the UKF filtering solution. However, since both the adaptive factor and equivalent weight factor are determined empirically, the improvement is limited.
iii) As expected, the resultant RMSEs by MLAUKF are significantly smaller than those of UKF and ARUKF due to its capability to track the real process noise covariance online. The achieved mean values of the RMSEs are at least 33% and 18% smaller than those by UKF and ARUKF, respectively.

Table 1
Means of the RMSEs of navigation errors obtained by UKF, ARUKF and MLAUKF during the time period from 100 s to 1000s.

		UKF	ARUKF	MLAUKF
Velocity(m/s)	East	0.0859	0.0752	0.0542
	North	0.0877	0.0755	0.0528
Position(m)	Longitude	5.7916	4.7432	3.8779
	Latitude	5.8324	4.7578	3.8312

Table 1 lists the mean values of the RMSEs for the horizontal velocity and position errors by the three filters during the time period from 100 s to 1000s. The statistical results in Table 1 also verify that MLAUKF have the better filtering accuracy than UKF and ARUKF in the presence of uncertainty involved in process noise covariance.

4.1.3. Computational performance

Trials were also conducted to investigate the computational performance of the proposed MLAUKF. The above Monte Carlo simulation trials were conducted with Matlab programs on a Pentium T4400 2.2 GHz PC with 2GB memory. Denote the average computational time (i.e. the filtering time for each run) of the UKF, ARUKF and MLAUKF as t_{UKF}, t_{ARUKF} and t_{MLAUKF}. We have $t_{UKF} = 612.4735s$, $t_{ARUKF} = 753.9062s$ and $t_{MLAUKF} = 704.5159s$. In order to eliminate the effect resulted from the difference of computers, a set of relative computational times is defined by

$$t^R_{UKF} = t_{UKF}/t_{UKF},\ t^R_{ARUKF} = t_{ARUKF}/t_{UKF},\ t^R_{MLAUKF} = t_{MLAUKF}/t_{UKF} \tag{60}$$

Apparently, $t^R_{UKF} = 1$. The calculated relative computational times of the three methods are shown in Fig. 5.

It can be seen from Fig. 5 that UKF has the smallest computational time among the above three filtering methods. The ARUKF computational time is 23.09% more than the UKF one. This is because ARUKF needs to determine the adaptive and robust factors at each time step during the filtering procedure. Compared with AURKF, MLAUKF also shows its superiority in terms of computational time. The computational time of MLAUKF is 6.55% smaller than that of AURKF, even though it is still slightly greater than that of UKF due to the estimation of the process

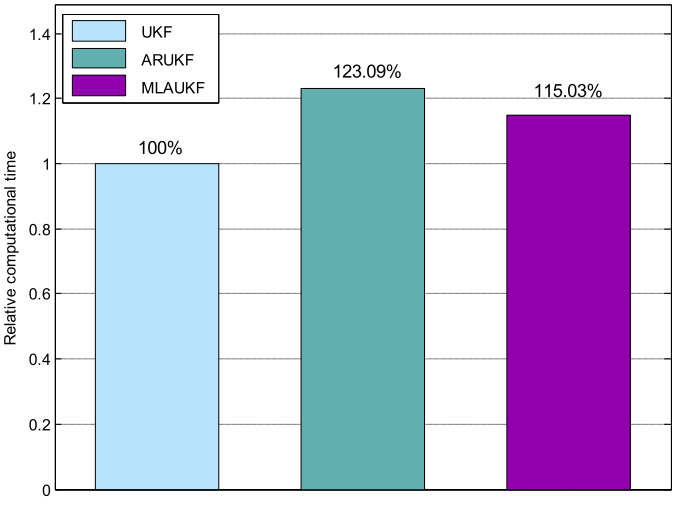

Fig. 5. Computational times of UKF, ARUKF and MLAUKF.

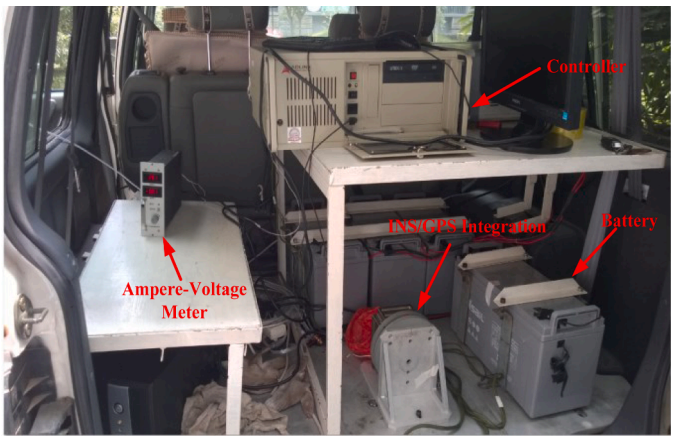

Fig. 6. Experimental car and navigation system components.

Fig. 7. Experimental car trajectory.

Table 2
Vehicular maneuvers.

Start and end times	Vehicular maneuvers	Time
0~150s	Static (start point)	150s
151~490s	Moving from the start point to the roundabout on the round hill road	340s
491~560s	Reverse turn at the roundabout on the round hill road	70s
561~860s	Moving from the roundabout to the end point on the round hill road	300s
861~970s	Static (end point)	110s

noise covariance. This demonstrates that the proposed MLAUKF has a faster computation speed than ARUKF, which is sufficient to achieve the real-time performance for vehicular INS/GPS integration.

4.2. Experiments and analysis

Practical vehicular navigation experiments were also conducted to evaluate the performance of the proposed MLAUKF. As shown in Fig. 6, the test car used a self-made INS/GPS integrated system for navigation. This navigation system includes a NV-IMU300 inertial measurement unit, and a JAVAD Lexon-GGD112T GPS receiver which offers the C/A GPS data at 1 Hz. Further, another JAVAD Lexon-GGD112T GPS receiver placed at a local reference station was used along with the one mounted on the vehicle to provide the differential GPS (DGPS) data at 1 Hz. Since DGPS can achieve the high positioning accuracy (less than 0.1 m) via post difference processing, the DGPS data are utilized as the reference for the comparison with the filtering results of the INS/GPS integration system.

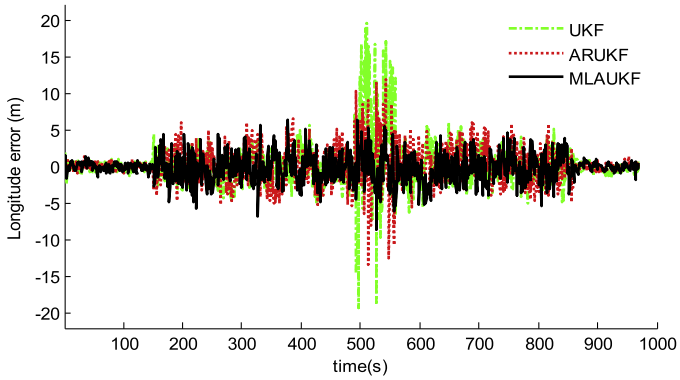

(a) Position error in longitude

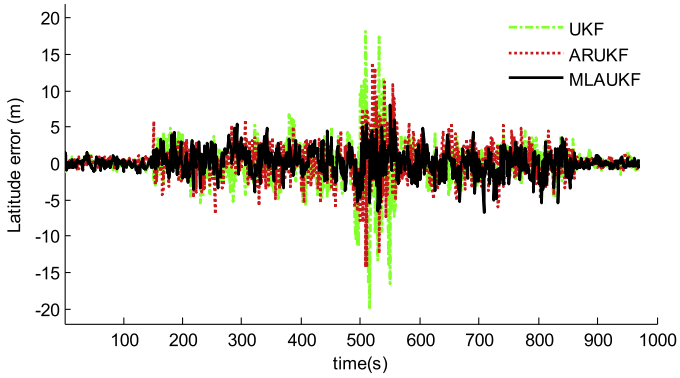

(b) Position error in latitude

Fig. 8. Horizontal position error obtained by UKF, ARUKF and MLAUKF for the practical experiment.

The vehicular navigation test was carried out near the Northwestern Polytechnical University (Xi'an, Shaanxi, China). The vehicular trajectory is shown in Fig. 7. The start position of the test car was at East longitude 108.775°, North latitude 34.030°, and altitude 419 m. The end position was East longitude 108.782°, North latitude 34.033°, and altitude 417 m. The test time was 970 s. Table 2 shows the various vehicular maneuvers. During the entire vehicular test process, the GPS works normally based on the signals received from at least seven satellites to provide credible navigation information, which means the uncertainty for INS/GPS integration mainly exists in the process noise [23]. The filtering period was 1 s. The estimation window size for the proposed MLAUKF was also set to $N = 25$. The initial parameters involved in the filters were set to be identical to the simulation case.

Fig. 8 shows the horizontal position errors of the car obtained by the UKF, ARUKF and MLAUKF. During the time periods 0~150 s and 861~970 s, the test car was static, with tiny disturbances of process

Table 3
MAE and STD of the horizontal position errors obtained by UKF, ARUKF and MLAUKF during the time period from 491 s to 560 s.

Methods		Horizontal position	
		Longitude	Latitude
UKF	MAE (m)	7.9487	7.1971
	STD (m)	8.5133	8.3349
ARUKF	MAE (m)	4.3201	5.0890
	STD (m)	5.3558	5.9405
MLAUKF	MAE (m)	2.7821	2.9270
	STD (m)	3.4197	3.6602

noise uncertainty. The horizontal position errors by the three methods are similar, which are within (−2.47 m, 2.51 m). During the time periods 151∼490 s and 561∼860 s, the car was moving smoothly on the round hill road, involving small disturbances of process noise uncertainty. The horizontal position errors of the three methods are still similar, which are within (−6.62 m, 6.84 m). However, during the time period 491∼560 s, the car was in a motion of reverse turn at the roundabout on the round hill road. Large disturbances of process noise uncertainty is involved in the process model (7) due to the severe maneuvers. Since UKF is sensitive to process noise uncertainty, its filtering solution is significantly disturbed, leading to the horizontal position error within (−19.93 m, 19.55 m). ARUKF weakens the disturbances of process noise uncertainty via the equivalent weighting and adaptive factors. However, as the equivalent weighting and adaptive factors are empirically determined, the improvement of accuracy is limited, leading to the horizontal position error within (−14.32 m, 13.86 m). In contrast, since the proposed MLAUKF restrains the disturbances of process noise uncertainty via online estimation of process noise covariance, its filtering accuracy is much higher than that of UKF and ARUKF, leading to the horizontal position error of (−8.59 m, 7.97 m).

Table 3 provides the mean absolute errors (MAEs) and standard deviations (STDs) of the three methods during the time period 491∼560 s. It can also be seen that the proposed MLAUKF has much smaller horizontal position error than the other two. This demonstrates the proposed MLAUKF can effectively restrain the disturbances of process noise uncertainty on the filtering solution, leading to improved filtering accuracy for vehicular INS/GPS integration.

5. Conclusions

This paper presents a new MLAUKF for vehicular INS/GPS integration in the presence of process noise uncertainty. The proposed MLAUKF estimates the process noise covariance using the designed ML estimator. Subsequently, it incorporates the estimations of process noise covariance in the adaptive filtering process to online update and adjust the Kalman gain matrix, leading to improved UKF robustness. Besides, the asymptotic convergence and unbiasedness of the ML estimator is proved, and the MLAUKF stability can be ensured with certain conditions. These all indicate that the proposed MLAUKF is promising to provide reliable filtering results for vehicular navigation. Monte Carlo simulations, experiments and comparison analysis with UKF and ARUKF verify that the proposed MLAUKF can effectively restrain the disturbances of process noise uncertainty on the filtering solution, leading to improved filtering accuracy for vehicular INS/GPS integration.

Future research work will focus on the improvement of the proposed MLAUKF. It is expected to combine with artificial intellegence technologies such as pattern recognition, neural network and advanced expert systems to improve the performance of INS/GNSS integration by automatically estimating process noise covariance.

Declaration of Competing Interest

None.

Acknowledgments

The work of this paper was supported by the Natural Science Basic Research Plan in Shaanxi Province of China (Project No: 2020JQ-234 & 2020JQ-150), the Aerospace Science and Technology Fund, the Fundamental Research Funds for the Central Universities (Project No. 3102018zy027) and the National Natural Science Foundation of China (Project No. 61703424 & 41904028).

Supplementary materials

Supplementary material associated with this article can be found, in the online version, at doi:10.1016/j.inffus.2020.08.005.

References

[1] D. Groves P, Principles of GPS, Inertial, and Multisensor Integrated Navigation Systems, Boston: Artech House, London, 2008.
[2] G. Hu G, S. Gao S, M Zhong Y, A derivative UKF for tightly coupled INS/GPS integrated navigation, ISA Trans 56 (2015) 135–144.
[3] G. Hu G, W Wang, Zhong YM .et al. A new direct filtering approach to INS/GNSS integration, Aerospace Science and Technology 77 (2018) 755–764.
[4] A. Noureldin, A. El-Shafie, M Bayoumi, GPS/INS integration utilizing dynamic neural networks for vehicular navigation, Information Fusion 12 (1) (2011) 48–57.
[5] H. Liu Y, Q. Fan X, C. Lv, et al., An innovative information fusion method with adaptive Kalman filter for integrated INS/GPS navigation of autonomous vehicles, Mech Syst Signal Process 100 (2018) 605–616.
[6] F. Sun, J Tang L, INS/GPS integrated navigation filter algorithm based on cubature Kalman filter, Control and Decision 27 (7) (2012) 1032–1036.
[7] Y. Cho S, IM-filter for INS/GPS-integrated navigation system containing low-cost gyros, IEEE Trans Aerosp Electron Syst 50 (4) (2014) 2619–2629.
[8] B. Cui B, Y. Chen X, H Tang X, Improved Cubature Kalman Filter for GNSS/INS Based on Transformation of Posterior Sigma-Points Error, IEEE Transactions on Signal Processing 65 (11) (2017) 2975–2987.
[9] G. Hu G, S. Gao S, M. Zhong Y, et al., Matrix weighted multisensor data fusion for INS/GNSS/CNS integration, Proceedings of the Institution of Mechanical Engineers, Part G: Journal of Aerospace Engineering 230 (6) (2016) 1011–1026.
[10] N. Chatzi E, A.W Smyth, Nonlinear system identification: particle-based methods, Encyclopedia of Earthquake Engineering (2014) 1–18.
[11] S. Gao S, G. Hu G, M Zhong Y, Windowing and random weighting-based adaptive unscented Kalman filter, Int J Adapt Control Signal Process 29 (2) (2015) 201–223.
[12] N. Chatzi E, A.W Smyth, The unscented Kalman filter and particle filter methods for nonlinear structural system identification with non-collocated heterogeneous sensing, Structural Control and Health Monitoring 16 (1) (2009) 99–123.
[13] Y. Shi, Z Han C, Adaptive UKF method with applications to target tracking, Acta Automatica Sinica 37 (6) (2011) 755–759.
[14] R. Astroza, H. Ebrahimian, P Conte J, Material parameter identification in distributed plasticity FE models of frame-type structures using nonlinear stochastic filtering, Journal of Engineering Mechanics 141 (5) (2014), 04014149.
[15] T. Kontoroupi, A.W Smyth, Online noise identification for joint state and parameter estimation of nonlinear systems, ASCE-ASME Journal of Risk and Uncertainty in Engineering Systems, Part A: Civil Engineering 2 (3) (2015), B4015006.
[16] J. Jwo D, F. Yang C, H. Chuang C, et al., Performance enhancement for ultra-tight GPS/INS integration using a fuzzy adaptive strong tracking unscented Kalman filter, Nonlinear Dyn 73 (1–2) (2013) 377–395.
[17] S. Yazdkhasti, Z. Sasiadek J, S Ulrich, Performance enhancement for GPS/INS fusion by using a fuzzy adaptive unscented Kalman filter. International Conference on Methods and Models in Automation and Robotics (MMAR), IEEE, 2016, pp. 1194–1199.
[18] S. Gao S, G. Hu G, M. Zhong Y, et al. Modified strong tracking unscented Kalman filter for nonlinear state estimation with process model uncertainty, Int J Adapt Control Signal Process 29 (12) (2015) 1561–1577.
[19] X. He, D. Wang Z, F. Wang X, et al., Networked strong tracking filtering with multiple packet dropouts: algorithms and applications, IEEE Transactions on Industrial Electronics 61 (3) (2014) 1454–1463.
[20] E. Soken H, C Hajiyev, Adaptive fading UKF with Q-adaptation: application to picosatellite attitude estimation, J Aerosp Eng 26 (3) (2011) 628–636.
[21] Y. Shi, Z Han C, Adaptive UKF method with applications to target tracking, Acta Automatica Sinica 37 (6) (2011) 755–759.
[22] B. Feng, Y. Fu M, B. Ma H, et al., Kalman filter with recursive covariance estimation –sequentially estimating process noise covariance, IEEE Transactions on Industrial Electronics 61 (11) (2014) 6253–6263.
[23] B. Chang L, L. Li K, Q Hu B, Huber's M-estimation based process uncertainty robust filter for integrated INS/GPS, IEEE Sens J 15 (6) (2015) 3367–3374.
[24] C. Jiang, B Zhang S, A Novel Adaptively-Robust Strategy Based on the Mahalanobis Distance for GPS/INS Integrated Navigation Systems, Sensors 18 (3) (2018) 695.
[25] Xian Z W., Hu X P., Lian J X. Robust innovation-based adaptive Kalman filter for INS/GPS land navigation. Chinese Automation Congress (CAC); 2013: 374–379.
[26] Y. Cho S, S Choi W, Robust positioning technique in low-cost DR/GPS for land navigation, IEEE Trans Instrum Meas 55 (4) (2006) 1132–1142.
[27] Q. Song, D Han J, An adaptive UKF algorithm for the state and parameter estimation of a mobile robot, Acta Automatica Sinica 34 (1) (2008) 72–79.
[28] Y. Meng, S. Gao S, M. Zhong Y, et al., Covariance matching based adaptive unscented Kalman filter for direct filtering in INS/GPS integration, Acta Astronaut 120 (2016) 171–181.
[29] X. Yang Y, B. He H, C Xu G, Adaptively robust filtering for kinematic geodetic positioning, J Geod 75 (2) (2001) 109–116.
[30] T. Wang Q, D. Xiao, Y Pang W, The research and application of Adaptive-Robust UKF on GPS/SINS integrated system, Journal of Convergence Information Technology 8 (6) (2013) 1169–1177.
[31] H. Mohamed A, K.P Schwarz, Adaptive Kalman filtering for INS/GPS, J Geod 73 (4) (1999) 193–203.
[32] P.D. Abramson, Simultaneous Estimation of the State and Noise Statistics in Linear Dynamical systems. PhD. Thesis, Massachusetts Institute of Technology, 1970.
[33] K Mehra R, Approaches to adaptive filtering, IEEE Trans Automat Contr 17 (5) (1972) 693–698.

[34] A. Gandhi M, L Mili, Robust Kalman filter based on a generalized maximum-likelihood-type estimator, IEEE Transactions on Signal Processing 58 (5) (2010) 2509–2520.
[35] K. Xiong, D. Liu L, Y Zhang H, Modified unscented Kalman filtering and its application in autonomous satellite navigation, Aerospace Science and Technology 13 (4) (2009) 238–246.
[36] X. Liu X, S. Xu X, T. Liu Y, et al., A method for SINS alignment with large initial misalignment angles based on Kalman filter with parameters resetting, Mathematical Problems in Engineering 2014 (2014) 1–11.
[37] K. Xiong, Y. Zhang H, W Chan C, Performance evaluation of UKF-based nonlinear filtering, Automatica 42 (2) (2006) 261–270.